COLEÇÃO

# DESAFIOS DAS ENGENHARIAS:

## ENGENHARIA DE COMPUTAÇÃO 2

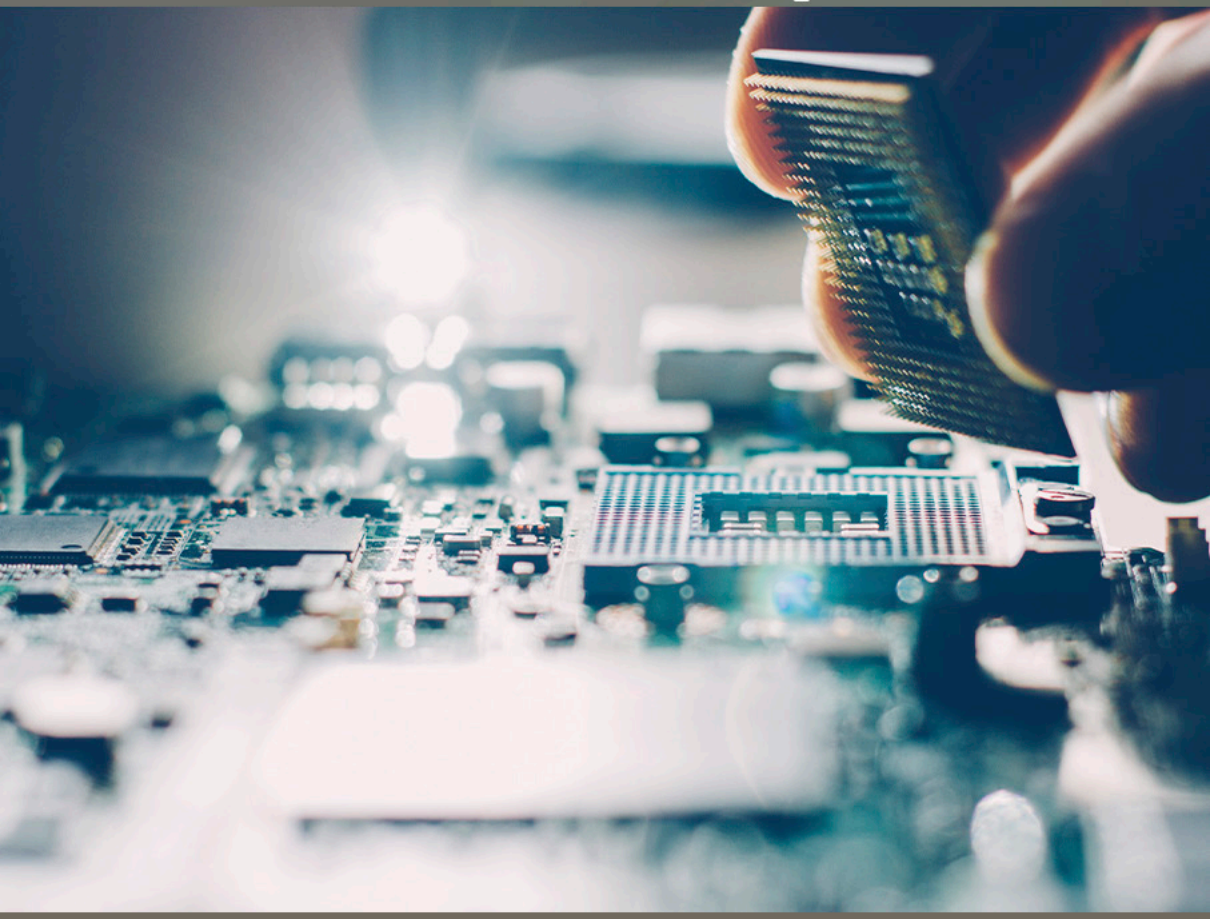

ERNANE ROSA MARTINS
(ORGANIZADOR)

Atena Editora
Ano 2021

COLEÇÃO

# DESAFIOS DAS ENGENHARIAS:

## ENGENHARIA DE COMPUTAÇÃO 2

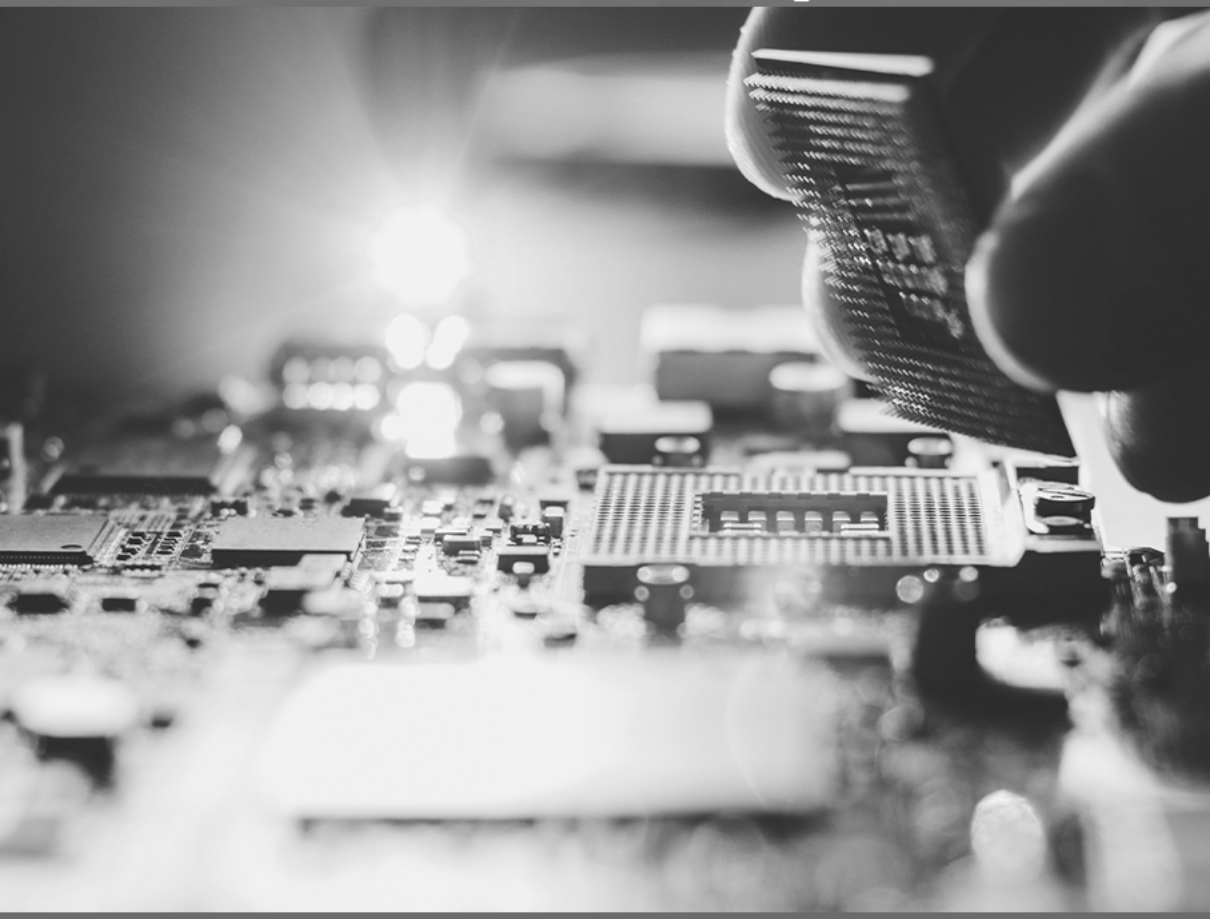

ERNANE ROSA MARTINS
(ORGANIZADOR)

Atena Editora
Ano 2021

**Editora chefe**
Profª Drª Antonella Carvalho de Oliveira
**Assistentes editoriais**
Natalia Oliveira
Flávia Roberta Barão
**Bibliotecária**
Janaina Ramos
**Projeto gráfico**
Natália Sandrini de Azevedo
Camila Alves de Cremo
Luiza Alves Batista
Maria Alice Pinheiro
**Imagens da capa**
iStock
**Edição de arte**
Luiza Alves Batista
**Revisão**
Os autores



Atena Editora
Ano 2021

**Ciências Agrárias e Multidisciplinar**



Atena Editora
Ano 2021

Atena Editora
Ano 2021

Atena Editora
Ano 2021

Coleção desafios das engenharias: engenharia de computação 2

**Diagramação:** Maria Alice Pinheiro
**Correção:** Giovanna Sandrini de Azevedo
**Indexação:** Gabriel Motomu Teshima
**Revisão:** Os autores
**Organizador:** Ernane Rosa Martins

**Dados Internacionais de Catalogação na Publicação (CIP)**

C691 Coleção desafios das engenharias: engenharia de computação 2 / Organizador Ernane Rosa Martins. – Ponta Grossa - PR: Atena, 2021.

Formato: PDF
Requisitos de sistema: Adobe Acrobat Reader
Modo de acesso: World Wide Web
Inclui bibliografia
ISBN 978-65-5983-384-9
DOI: https://doi.org/10.22533/at.ed.849211808

1. Engenharia da computação. I. Martins, Ernane Rosa (Organizador). II. Título.

CDD 621.39

**Elaborado por Bibliotecária Janaina Ramos – CRB-8/9166**

**Atena Editora**
Ponta Grossa – Paraná – Brasil
Telefone: +55 (42) 3323-5493
www.atenaeditora.com.br
contato@atenaeditora.com.br

Atena Editora
Ano 2021

*Ciências Exatas e da Terra e Engenharias*

## DECLARAÇÃO DOS AUTORES

Os autores desta obra: 1. Atestam não possuir qualquer interesse comercial que constitua um conflito de interesses em relação ao artigo científico publicado; 2. Declaram que participaram ativamente da construção dos respectivos manuscritos, preferencialmente na: a) Concepção do estudo, e/ou aquisição de dados, e/ou análise e interpretação de dados; b) Elaboração do artigo ou revisão com vistas a tornar o material intelectualmente relevante; c) Aprovação final do manuscrito para submissão.; 3. Certificam que os artigos científicos publicados estão completamente isentos de dados e/ou resultados fraudulentos; 4. Confirmam a citação e a referência correta de todos os dados e de interpretações de dados de outras pesquisas; 5. Reconhecem terem informado todas as fontes de financiamento recebidas para a consecução da pesquisa; 6. Autorizam a edição da obra, que incluem os registros de ficha catalográfica, ISBN, DOI e demais indexadores, projeto visual e criação de capa, diagramação de miolo, assim como lançamento e divulgação da mesma conforme critérios da Atena Editora.



Atena Editora
Ano 2021

## DECLARAÇÃO DA EDITORA

A Atena Editora declara, para os devidos fins de direito, que: 1. A presente publicação constitui apenas transferência temporária dos direitos autorais, direito sobre a publicação, inclusive não constitui responsabilidade solidária na criação dos manuscritos publicados, nos termos previstos na Lei sobre direitos autorais (Lei 9610/98), no art. 184 do Código penal e no art. 927 do Código Civil; 2. Autoriza e incentiva os autores a assinarem contratos com repositórios institucionais, com fins exclusivos de divulgação da obra, desde que com o devido reconhecimento de autoria e edição e sem qualquer finalidade comercial; 3. Todos os e-book são *open access, desta forma* não os comercializa em seu site, sites parceiros, plataformas de *e-commerce,* ou qualquer outro meio virtual ou físico, portanto, está isenta de repasses de direitos autorais aos autores; 4. Todos os membros do conselho editorial são doutores e vinculados a instituições de ensino superior públicas, conforme recomendação da CAPES para obtenção do Qualis livro; 5. Não cede, comercializa ou autoriza a utilização dos nomes e e-mails dos autores, bem como nenhum outro dado dos mesmos, para qualquer finalidade que não o escopo da divulgação desta obra.



Atena Editora
Ano 2021

## APRESENTAÇÃO

A Engenharia de Computação é a área que estuda as técnicas, métodos e ferramentas matemáticas, físicas e computacionais para o desenvolvimento de circuitos, dispositivos e sistemas. Esta área tem a matemática e a computação como seus principais pilares. O foco está no desenvolvimento de soluções que envolvam tanto aspectos relacionados ao software, quanto à elétrica/eletrônica. Os profissionais desta área são capazes de atuar principalmente na integração entre software e hardware, tais como: automação industrial e residencial, sistemas embarcados, sistemas paralelos e distribuídos, arquitetura de computadores, robótica, comunicação de dados e processamento digital de sinais.

Dentro deste contexto, esta obra aborda diversos aspectos tecnológicos computacionais, tais como: implementação e modificações numéricas a serem feitas no algorítmo de Anderson (2010) para simular o escoamento sobre uma asa finita submetida a ângulos de ataque próximos ao estol; modelo distribuído para analisar a influência da formação e do adensamento de geada sobre o desempenho de evaporadores do tipo tubo-aletado, comumente usados em refrigeradores frost-free; um algoritmo de Redes Neurais Convolucionais(CNN) que identifica se a pessoa está ou não utilizando a máscara; potencialidades do M-Learning e Virtual Reality no curso técnico em Agropecuária; avaliação da qualidade da energia elétrica em um sistema de geração de energia fotovoltaica; uma abordagem para a segmentação de imagens cerebrais, utilizando o método baseado em algoritmos genéticos pelo método de múltiplos limiares; estudo numérico de uma âncora torpedo sem aletas cravada em solo isotrópico puramente coesivo, utilizando um modelo axissimétrico não-linear em elementos finitos; estudo acerca da análise numérica de placas retangulares por meio do método das diferenças finitas, obtendo soluções aproximadas para o campo de deslocamentos transversais bem como os correspondentes momentos fletores, para problemas envolvendo uma série de condições de contorno, utilizando-se o software Matlab® para simulação; desenvolvimento e aplicação da Realidade Virtual (RV) como Tecnologia de Informação e Comunicação (TIC) para auxiliar no processo de ensino-aprendizado de disciplinas do Ensino Médio; avaliação dos resultados obtidos em campanhas de medição de qualidade da energia elétrica (QEE) na rede básica em 500 kV; examinar o comportamento mecânico-estático de uma longarina compósita projetada para uma aeronave esportiva leve através de investigações numéricas, empreendidas em software (ANSYS Release 19.2) comercial de elementos finitos; construção de um sistema para monitoramento de ativos públicos; a relação da Sociedade 5.0 envolvida no contexto da Indústria 4.0 e a Transformação Digital; algoritmos de seleção e de classificação de atributos, identificando as vinte principais características que contribuem para o desempenho alto ou baixo dos estudantes; a Mask R-CNN, utilizada para a segmentação de produtos automotivos (parabrisas, faróis, lanternas, parachoques e retrovisores) em uma empresa do ramo de reposição automotiva; o nível de usabilidade do aplicativo protótipo

para dispositivo móvel na área da saúde voltado ao auxílio do monitoramento móvel no uso de medicamentos em seres humanos.

Sendo assim, está obra é significativa por ser composta por uma gama de trabalhos pertinentes, que permitem aos seus leitores, analisar e discutir diversos assuntos importantes desta área. Por fim, desejamos aos autores, nossos mais sinceros agradecimentos pelas significativas contribuições, e aos nossos leitores, desejamos uma proveitosa leitura, repleta de boas reflexões.

Ernane Rosa Martins

## SUMÁRIO

# CAPÍTULO 11

# ANÁLISE NUMÉRICA DA CAPACIDADE DE CARGA DE ÂNCORAS TORPEDO CONSIDERANDO EFEITOS DE SETUP

*Data de aceite: 02/08/2021*
*Data de submissão: 05/05/2021*

**Guilherme Kronemberger Lopes**
Department of Civil Engineering, Federal University of Rio de Janeiro
Rio de Janeiro – Rio de Janeiro
http://lattes.cnpq.br/5270566094871046

**José Renato Mendes de Sousa**
Department of Civil Engineering, Federal University of Rio de Janeiro
Rio de Janeiro – Rio de Janeiro
http://lattes.cnpq.br/3211660196134627

**Gilberto Bruno Ellwanger**
Department of Civil Engineering, Federal University of Rio de Janeiro
Rio de Janeiro – Rio de Janeiro
http://lattes.cnpq.br/2639351643523334

**RESUMO**: A âncora torpedo possui formato de "foguete" e sua instalação á dada através de queda livre, utilizando seu próprio peso como energia cinética de cravação. O processo de cravação induz a geração de um excesso de poro-pressões e causa perturbações e cisalhamentos excessivos, afetando as tensões, deformações e propriedades de resistência do solo no entorno da âncora. Imediatamente após a instalação, a capacidade da carga da âncora é significativamente reduzida. No entanto, após a cravação, observa-se que a capacidade de carga aumenta com o tempo, num processo conhecido como setup. Este artigo apresenta um estudo numérico de uma âncora torpedo sem aletas cravada em solo isotrópico puramente coesivo, utilizando um modelo axissimétrico não-linear em elementos finitos. O modelo de plasticidade de "Cap" foi escolhido para descrever o comportamento constitutivo do solo. A interação solo-âncora é simulada usando pares de contato do tipo superfície-superfície, com propriedade de contato do tipo penalidade. As análises numéricas foram conduzidas utilizando o software Abaqus/CAE. Os resultados obtidos com este modelo indicaram que a permeabilidade do solo tem um papel importante no processo de setup. Além disso, os parâmetros investigados do modelo constitutivo do solo apresentaram um padrão de comportamento na resposta da estrutura.
**PALAVRAS - CHAVE**: Âncoras torpedo, Elementos finitos, Setup.

## NUMERICAL ANALYSIS OF THE HOLDING CAPACITY OF TORPEDO ANCHORS CONSIDERING SETUP EFFECTS

**ABSTRACT**: The torpedo anchor has a "rocket" shape, and its installation is given by free fall using heavyweights as the driving kinetic energy. Its driving process induces an excess pore water pressure generation and causes significant shearing and disturbance, which affects the stress, strain, and strength characteristics of the soil surrounding the anchor. Immediately after installation, the holding capacity of the torpedo anchor is significantly reduced. Although, after the anchor driving, holding power is observed to increase with time in a process referred to as

setup. This paper presents a numerical-based study of a finless torpedo anchor embedded in a purely cohesive isotropic soil using an axisymmetric nonlinear finite element model. The plasticity Cap model was chosen to describe the mechanical behavior of the soil. Anchor-soil interaction is simulated using surface-to-surface contact pairs with a penalty-type contact property. Several analyses are conducted using the software Abaqus/CAE. The results obtained with this model indicated that soil permeability plays an essential role in the setup process. Furthermore, plasticity parameters are also investigated, and the results present a pattern of behavior of the structure's response.
**KEYWORDS**: Torpedo anchors, Finite element, setup.

## 1 | INTRODUCTION

The world's great demand for oil and gas has stimulated new researches focused on offshore structures design. Due to the innovative nature of the equipment employed by the offshore oil industry, the exploitation of oil and gas is available for water depths over 3,000 meters. According to Ehlers *et al*. (2004), some typical foundations employed by the offshore industry are suction anchors, vertical load anchors (VLAs), and suction embedded plate anchors (SEPLAs). Although, the installation costs of these anchors surprisingly increases with water depth.

In this scenario, Wodehouse *et al*. (2007) describe that the torpedo anchor has proven to be an outstanding alternative in Brazilian offshore fields. Additionally, according to Medeiros Jr. (2002), this type of anchor has low construction and installation costs, not dependent on water depth, and withstands high vertical loads. The torpedo anchor (Fig. 1) belongs to the group named dynamically installed anchors (DIAs). Besides the torpedo anchors, the existing DIAs also include OMNI-Max anchors and deep penetrating anchors (DPAs).

The torpedo anchor has a rocket shape with a varying number of flukes. Its installation is given by free fall from a designated height above the seabed using heavyweights as the driving kinetic energy. Its structure usually comprises four different components: a padeye that connects the first chain segment of the mooring line to the anchor; a ballasted shaft of carbon steel; a varying number of flukes, usually from 0 up to 4; and a conical tip that is designed to help the embedment of the anchor. Typical torpedo anchor's weight varies from 35 tons up to 98 tons (Sousa *et al*., 2011).

Figure 1. Typical torpedo anchor with four flukes: conical tip (left) and top view with detail of the padeye (right) (Sousa et al., 2011).

After a torpedo anchor is driven in saturated soil, the pullout resistance is often observed to increase with time. This phenomenon is referred to as setup. Although the exact mechanism is not entirely understood (Komurka *et al*. 2003, Simulia 2007, Houssain *et al*., 2014), two processes are believed to play an important role. The first of them corresponds to an increase in the soil's effective stresses associated with the dissipation of the excess pore pressure built up around the anchor during installation. The other one is related to thixotropic bonding between the soil grains and some aging effects.

Some investigations about the setup process of driven DIAs have been carried out in the past few years. Hossain *et al*. (2015) performed centrifuge tests for torpedo anchors and reported that approximately 80% of the long-term anchor capacity would be available within one year after anchor installation. Raie and Tassoulas (2016) and Radgahar *et al*. (2015) performed numerical analyses of finless torpedo anchors. They observed that the time needed to achieve a consolidation ratio of 90% is considerably lower than the total time required to achieve complete consolidation of the soil. Richardson *et al*. (2009) reported that 50% of the holding capacity of the DIA is achieved over 35 to 350 days after installation. Moreover, 90% of the operational holding capacity is achieved over 2.4 to 24 years. In general, the authors emphasize that these values are highly dependent on the soil properties where the anchor have been installed.

Regarding the project and design of torpedo anchors, setup effects are not directly incorporated. Sousa *et al*. (2011) mention that, in practice, a typical torpedo anchor is first loaded approximately three months after its installation. Still, the imposed loads are much lower than its load capacity, as safety factors between 1.5 and 2.0 are employed in the anchor's design. Hence, there is still a gap of information concerning the setup mechanism in the anchor's design.

Therefore, to contribute to this task, a nonlinear axisymmetric finite element (FE) model is proposed. A finless torpedo anchor embedded in a purely cohesive isotropic soil

is analyzed. The anchor is assumed to be “wished in place,” and that soil initial stress conditions can be obtained immediately after installation, using the Cavity Expansion Method (CEM). All analyses were carried out using Abaqus/CAE® (2013). The proposed FE model is described in detail before presenting the results of a parametric study obtained using this model.

## 2 | FINITE ELEMENT MODELING

### 2.1 Soil Modeling

The soil is modeled by a conventional approach that considers the porous medium as a multiphase material and adopts the effective stress principle (Terzaghi, 1936) to describe its behavior. The soil is considered fully saturated, and the wetting liquid is seawater. The porous medium is modeled by attaching the finite element mesh to the solid phase, and the fluid present inside the medium can flow through this mesh.

A continuity equation is required for the fluid inside the soil, equating the rate of increase in the liquid mass stored to the rate of mass of liquid flowing into the point within the time increment. This continuity statement is written in a variational form as a basis for finite element approximation, which is defined as:

$$\int_V \frac{1}{J}\frac{d}{dt}(J\rho_w n_w)dV = -\int_S \rho_w n_w \mathbf{n}\cdot\mathbf{v}_w dS \qquad (1)$$

where $J$ is the ratio of the medium’s volume in the current configuration to its volume in the reference configuration, $p_w$ is the density of seawater, $n_w$ is the volume ratio of free wetting liquid at a point, $n$ is the outward normal to $S$, and $v_w$ is the seepage velocity.

The seawater flow through the solid phase of the soil is supposed to be described by Darcy’s law. Darcy’s law states that, under uniform conditions, the volumetric flow rate of the wetting liquid through a unit area of the medium, $snv_w$, is proportional to the negative of the gradient of the piezometric head, thus:

$$sn\mathbf{v}_w = -\hat{\mathbf{k}}\cdot\frac{\partial\phi}{\partial\mathbf{x}} \qquad (2)$$

where $s$ is the saturation, $n$ is the porosity of the porous medium, $\hat{\mathbf{k}}$ is the permeability of the medium, and $\phi$ is the piezometric head.

The modified Drucker-Prager (DP) plasticity model, commonly referred to as Cap model, was chosen to represent the nonlinear material behavior. According to Helwany (2010), this model is appropriate to describe soil behavior because it can consider the effects of stress history, stress path, dilatancy, and the intermediate principal stress. The yield surface of this plasticity model consists of three parts: a DP shear failure ($Fs$), an elliptical cap ($Fc$), and a smooth transition region between the shear failure and the cap ($Ft$),

as shown in Fig. 2.

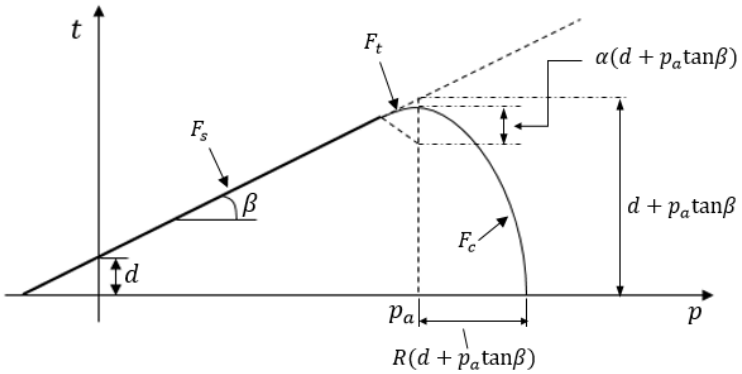


Figure 2. Yield surfaces of the Cap model in the p-t plane.

In this study, the hardening-softening behavior of the Cap model is simply described by a piecewise linear function relating the mean effective (yield) stress, *p'*, and the volumetric plastic strain, $\varepsilon^{p}_{v}$. More details about this constitutive model are described by Helwany (2010) and Abaqus Online Documentation (2013).

## 2.2 Soil FE Mesh Characteristics

The undrained response of a torpedo anchor embedded in clay is a classical elastoplastic problem. It requires no locking for incompressible materials and good bending behavior to obtain acceptable answers (Sousa *et al.*, 2011). Therefore, it was chosen to use 8-noded solid isoparametric axisymmetric elements to represent the soil. Additionally, these elements can account for an extra degree of freedom to save pore pressure values.

An overview of the main dimensions of the soil mesh is shown in Fig. 3. The height of the cylinder is given by the sum of the embedment depth of the anchor ($H_p$), the length of the anchor ($H_c$) and the distance of the tip of the torpedo to the bottom of the FE mesh ($H_a$). According to Sousa *et al.*, a diameter of 20D$\alpha$ for the soil cylinder and a distance of 5 m for $H_a$ dimension was enough to simulate an “infinite” media. Hence, these values were also considered in all analyses performed throughout this study.

The elements have dimensions varying between 0.10m and 0.25m in the regions where high plastic strains are expected to occur (close to the anchor) and between 0.25m and 0.50m in the areas far from the anchor shown in Fig. 3. These dimensions were adopted after a mesh study was performed, where the results indicated that a more refined mesh did not present significant differences in the anchor response.

Regarding the boundary conditions, the vertical and horizontal displacements of the soil cylinder are restrained at the nodes associated with its base. Displacements in the

radial direction of the nodes associated with the outer wall of the cylinder are restrained.

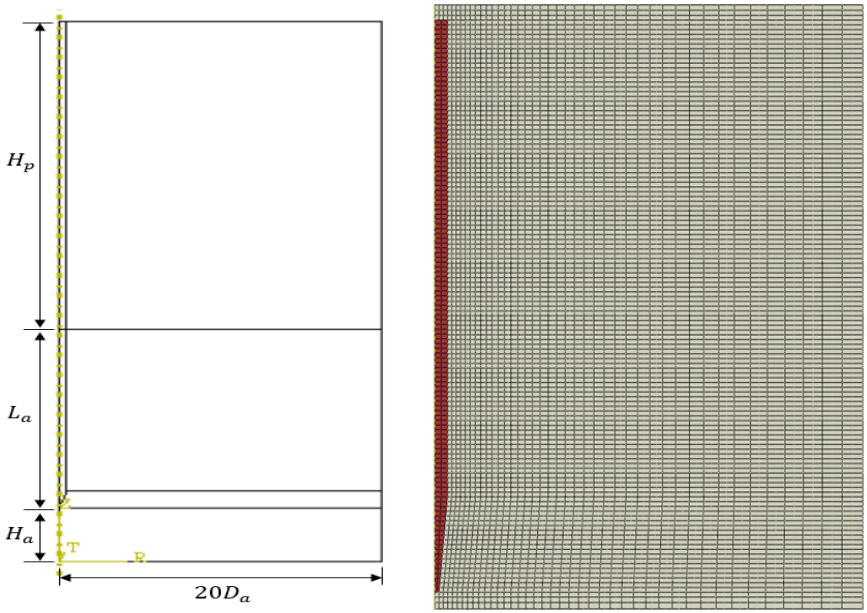


Figure 3. General view of the FE model.

## 2.3 Anchor modeling

The torpedo anchor is modeled with isoparametric solid elements analogous to the ones used to represent the soil but without the pore pressure degree of freedom. It is worth mentioning that neither the padeye at the top of the anchor nor the mooring line are represented in the proposed model. Hence, the load from the mooring line is applied at a node placed 1m above the top of the anchor, and it is rigidly connected to the top of the anchor by rigid bars using the beam MPC (Multiple Point Constraint) options in Abaqus (2013), as presented in Fig. 4.

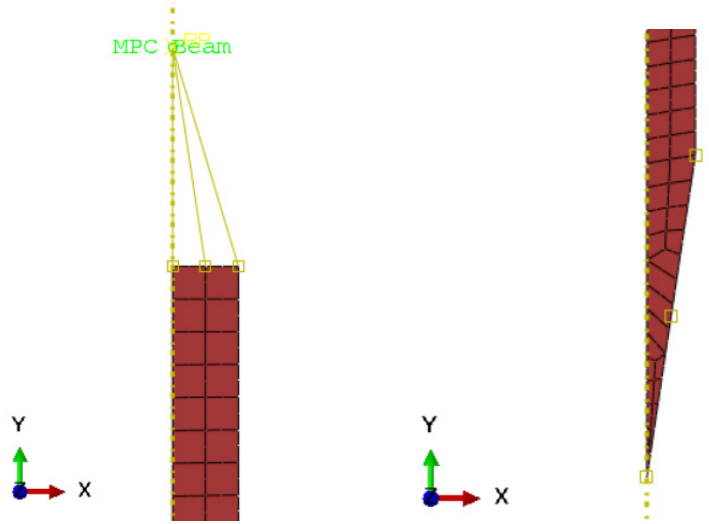


Figure 4. FE mesh details of the finless torpedo anchor: top view and load application (right) and bottom part of the tip (left).

Anchor loading is simulated by applying a concentrated force on the reference node at a rate of 10,000 kN/s. This extremely high rate of loading is employed to ensure that the soil will behave in undrained conditions.

## 2.4 Anchor-soil interaction

The anchor-soil interaction is simulated using the surface-to-surface master/slave contact pairs. The slave surface is constrained against penetrating the master surface and, usually defined as the softer one. In the proposed model, as the anchor is much stiffer than the surrounding soil, all master elements are placed on the outer wall of the anchor, and all slave elements are on the surrounding soil contact surface.

Another critical aspect of the analysis is permeation between the materials: if there will be or not fluid flow between them. As the pore pressure degree of freedom is only active on the soil elements, the FE program automatically considers the contact surface as impermeable; hence, no fluid flow will occur between the materials.

The interaction between the anchor and the soil is simulated using a penalty-type interface, in which the main parameter is the friction coefficient between the surfaces in contact. According to Helwany (2010), this kind of interface can describe the frictional interaction between the anchor surface and the surrounding soil in touch.

Karlsrud (2012) states that pile axial loading capacity can be obtained by calculating the shear resistance over the pile shaft concerning time and effective radial stress. The author assumes that the effective radial stress over the pile can be multiplied by a factor, $f_{cons}$, varying between 0.2 and 0.4, according to the following equation:

$$f_{cons} \cdot \sigma'_r(U) = s_u(U) \quad (5)$$

where $\sigma'_r(U)$ is the effective radial stress as a function of the soil degree of consolidation and $s_u$ is the soil undrained shear strength.

However, during the analyses, it was observed that when a factor equals 0.2 was applied to the results corresponding to effective radial stress at 100% consolidation, the values obtained were much higher than those of the soil with intact undrained shear strength. Thus, to bypass this problem, the factor was calibrated against the undrained shear strength corresponding to the soil fully reconsolidated. In this case, it was assumed that the undrained shear strength of the fully reconsolidated soil is equal to the one recommended by the α-method from API (2005). Hence, the calibrated friction factor is given by:

$$f_{cons\_calib} = \frac{\alpha \cdot s_u}{\sigma'_r(U = 100\%)} \quad (6)$$

## 2.5 Initial stress state of the soil

An essential aspect of the torpedo anchor analysis is the simulation of the initial stress state of the soil, *i.e.*, the stresses before the application of any structural load. As the proposed FE model does not simulate the anchor penetration in the soil, stress changes in the soil surrounding the anchor are therefore claimed to be similar to those produced from the expansion of an ideal cylindrical cavity.

The Cavity Expansion Method (CEM) assumes that the strains induced from the anchor installation come from an ideal expansion of a cylindrical cavity. Randolph and Wroth (1979) present a solution based on the assumption of a cylindrical cavity in a perfectly elastoplastic (EP) type soil model. They assume axial symmetry and plane strain conditions, implying that only radial displacement of soil particles will occur.

Hill (1950) and Gibson and Anderson (1961) demonstrate the expressions for the stresses around an expanded cavity. For a cavity expanded from zero radii to a radius $r_0$, the radial and circumferential stress changes within the plastic zone are given respectively by:

$$\Delta\sigma_r = s_u \left[1 + ln\left(\frac{G_{50}}{s_u}\right)\right] \quad (7)$$

$$\Delta\sigma_\theta = s_u \left[-1 + ln\left(\frac{G_{50}}{s_u}\right)\right] \quad (8)$$

The relationship between $G_{50}$ and $s_u$ can be estimated by the following empirical expression (Keaveny and Mitchell, 1986):

$$\frac{G_{50}}{s_u} = \frac{e^{\left(\frac{137-\mathrm{IP}}{23}\right)}}{\left[1+\ln\left(1+\frac{(\mathrm{OCR}-1)^{3.2}}{26}\right)\right]^{0.8}} \quad (9)$$

where $IP$ is the plasticity index of the soil and $OCR$ is the overconsolidation ratio of the soil.

Further, Randolph and Wroth (1979) estimate the excess pore pressure by assuming that the mean effective stress remains constant under undrained conditions. This initial distribution is such that the pore pressure is maximal at the anchor-soil interface and diminishes exponentially with radial distance from the center of the anchor. The distribution of the initial excess pore pressure can then be written as:

$$\Delta u_0 = \begin{cases} 2s_u(z)ln\left(\frac{r_p}{r}\right), & r_0 \le r \le r_p \\ 0, & r > r_p \end{cases} \quad (10)$$

where $s_u(z)$ is the soil undrained shear strength varying with depth, $r_p$ is the plasticized radius of the disturbed soil after anchor driving, and $r_0$ is the anchor radius.

In theory, the expansion of a cylindrical cavity is modeled with an initial radius of zero. In contrast, numerical calculations must begin with a finite cavity radius to avoid infinite circumferential strains. Carter *et al*. (1979) found that doubling the cavity radius is adequate for EP and modified Cam Clay models. Thus expanding a cavity from $a_0$ to $a_0$ can approximate the cavity expansion from $r = 0$ to $r_0$, i. e. model the installation of an anchor with a shaft radius of $r_0$. Though, for the analyses conducted in this study, it was considered a relationship of $a_0 = 0.5r_0$.

## 2.6 Solution procedure

A typical FE mesh to predict the load capacity of a finless torpedo anchor considering setup effects has approximately 15,000 elements and 100,000 degrees of freedom. Complete setup analysis is run, basically, in three consolidation steps. In the first one, the initial stress state of the soil is imported to the present model from a previous analysis where the CEM is simulated following the steps described by Lopes [23]. Briefly, the process consists of modeling the undisturbed soil with the in situ stress, removing part of the soil, and placing a rigid bar into it, creating a cylindrical cavity. Thus, the bar is forced to move against the soil wall, as shown in Fig. 5, simulating the expansion of a cylindrical cavity.

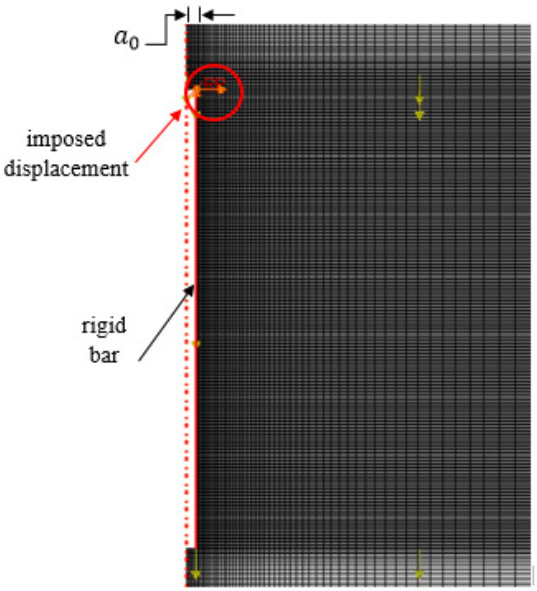


Figure 5. Detail of the rigid bar and its imposed displacement represents the CEM simulation (adapted from Lopes, 2019).

The first step is kept short to properly simulate the soil conditions immediately after anchor driving, not allowing the soil to consolidate (0.001s, for instance). The second step involves continuing consolidation analysis for lengths of time varying from 10 seconds up to 100 million seconds (approximately 3.2 years). In this step, the excess pore pressure dissipates as time progresses while the soil simultaneously consolidates. Finally, the third step involves assessing the pullout strength by applying a concentrated force at the reference node positioned above the top of the anchor and monitoring the vertical motion.

## 3 I PARAMETRIC STUDY

### 3.1 Description

In this paper, various FE analyses were performed to study the importance of setup effects on the holding capacity of a finless torpedo anchor. Additionally, four parameters were varied to understand their influence on setup analysis: (i) permeability coefficient of the soil, (ii) cap eccentricity parameter, (iii) cap transition surface parameter, and (iv) flow stress ratio.

The soil has an elastic modulus of 68.9 MPa, a Poisson ratio of 0.3, and a dry density of 1100 kg/m³. Cap model, with cohesion ($d$) of 0 kPa, friction angle ($\beta$) of 50.2°, cap eccentricity ($R$) of 0.4, transition surface radius ($\alpha$) of 0.5, and flow stress ratio ($K$) of 1.0, is used for describing soil plasticity. The existence of a cap limits the amount of dilation when

the soil gets deformed in shear. Permeability of the soil was set initially to 2.5e-10 m/s, and an initial void ratio of 1.5 was considered in all analyses.

The finless torpedo anchor is considered to behave elastic with a Young modulus of 15 GPa and a Poisson ratio of 0.3. The main dimensions of the torpedo anchor analyzed are presented in Fig. 6, and, for all analyses, the submerged weight of the torpedo anchor was assumed to be equal to 650 kN.

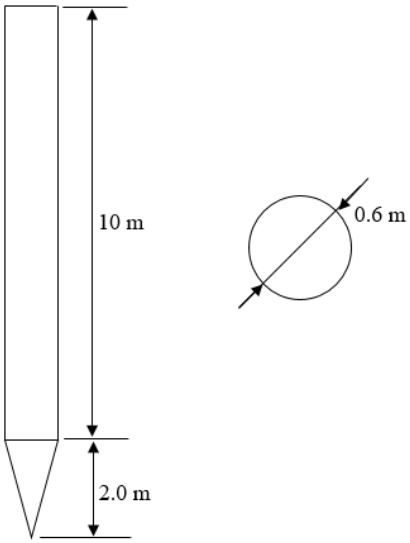


Figure 6. Main dimensions of the finless torpedo anchor.

It is worth mentioning that in this work, the anchor is supposed to be installed perfectly vertically, while, in practice, inclinations concerning the horizontal plane are often observed. Moreover, a unique embedment depth of 15 m was assumed in all analyses. A further investigation on these assumptions is presented by Lopes (2019).

### 3.2 Setup effects

The influence of setup effects on the holding capacity of torpedo anchors can be observed in Fig. 7. The anchor's pullout resistance is plotted for different instants of time after driving, varying from 10 seconds (simulating the scenario right after installation) and 10 years. Force vs. displacement curves are normalized concerning anchor's weight, $W_a$, and anchor's external diameter (shaft diameter), $D_a$, respectively.

As expected, the anchor experiences an increase in its holding capacity, whereas setup time increases. In general, the holding capacity of the finless torpedo anchor analyzed increases at a high rate for the first days after anchor installation, and this rate decreases as time progresses. Notice that the relationship between the holding capacity of the anchor, *Q*, and the anchor's weight had an increase of approximately 32% comparing the results for setup times of 0 days and 10 years.

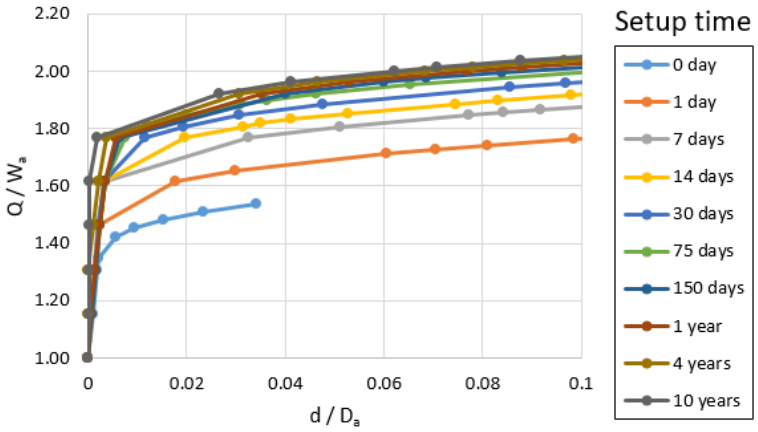


Figure 7. Torpedo anchor's normalized pullout capacity considering setup effects.

Fig. 8 presents the setup curve for the torpedo anchor analyzed. The vertical axis shows the values of the normalized holding capacity of the anchor, which is the holding capacity at a time *t* after driving to the holding capacity immediately after driving ($t = 0$). Two main phases of setup can be observed in Fig. 8. The first one, with a linear rate of dissipation of excess pore pressure to the log of time, comprising consolidation times ranging from 1 to 150 days after driving; and the second, for consolidation times over 150 days.

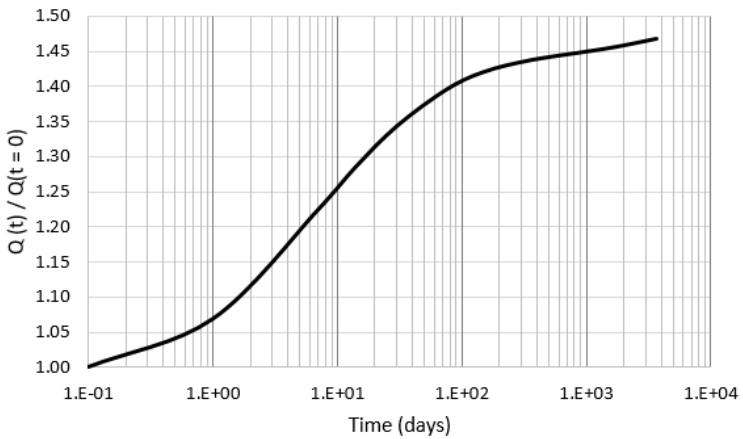


Figure 8. Torpedo anchor's setup curve.

The exact influence of the first instants of time of setup was not well reproduced by the numerical analyses. Hence, no further conclusions could be made concerning this phase.

The results shown in Fig. 8 indicate that, for the present problem, the holding

capacity of the torpedo anchor will be almost 50% higher after complete soil consolidation when comparing to the holding power at the end of driving. These results emphasize the importance of considering the setup effects on the project of torpedo anchors.

### 3.3 Permeability coefficient effects

Fig. 9 shows soil consolidation ratio curves considering different permeability coefficients for an element of soil located on the soil-anchor interface corresponding to the midpoint of the anchor shaft (5 m above the top of the anchor). Soil consolidation ratio is defined as:

$$U(t) = 1 - \frac{\Delta u(t=0)}{\Delta u(t)} \tag{11}$$

where $\Delta u$ (t = 0) is the excess pore pressure immediately after anchor installation and $\Delta u(t)$ is the excess pore pressure at a time *t*.

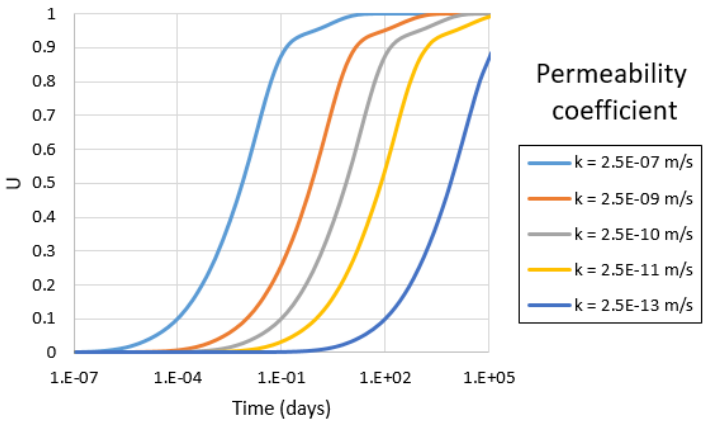


Figure 9. Consolidation ratio curves for different soil permeability coefficients.

Looking through the results presented in Fig. 9, it can be noticed that the time needed to achieve a higher consolidation ratio of the soil increases exponentially as time progresses. Also, comparing the different soil consolidation curves, it can be observed that if the permeability coefficient of the soil is decreased by one order of magnitude, then the soil consolidation ratio increases an order of magnitude. The same behavior can be observed when increasing or decreasing more than one order of the permeability coefficient. It is essential to observe that the values are not precisely the same as those multiplied by a factor of 10, but the expected results are very close to that.

### 3.4 Cap model parameters effects

According to Helwany (2010), to ensure convexity of the yield surface, the range

$0.778 \leq K \leq 1.0$ should not be violated. Effects of different values of $K$ on anchor's holding capacity are presented in Fig. 10. The results indicated that the parameter $K$ has a low influence on the anchor response. It is emphasized that analysis convergence is achieved with fewer iterations when a value of $K$ = 1.0 is used.

The transition surface parameter, $\alpha$, is generally a small number used to define a smooth transition surface between the Drucker-Prager shear failure surface and the cap surface. Fig. 11 shows the effects of different values of the transition surface parameter on anchor's holding capacity.

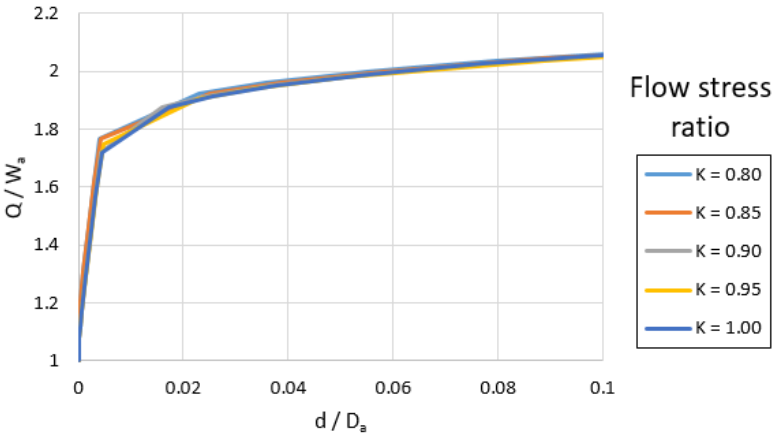


Figure 10. Influence of different flow stress ratios on pullout capacity.

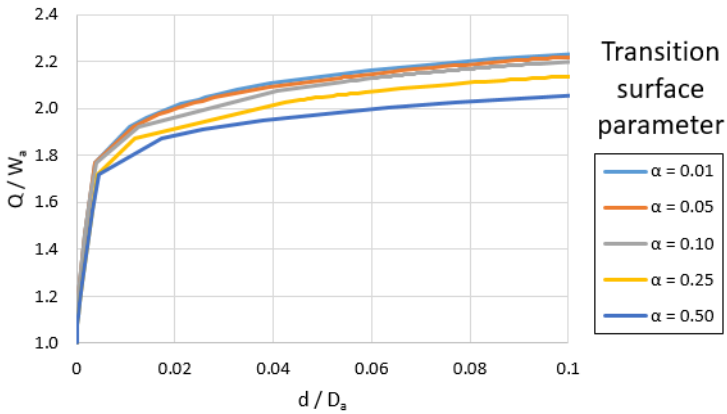


Figure 11. Influence of transition surface parameter on pullout capacity.

Fig. 11 indicates that the curves converge for small values of the cap transition surface parameter. On the other hand, when higher values of this parameter are adopted,

the response seems more conservative. In addition, it is emphasized that numerical convergence is achieved with fewer iterations for small values of this parameter (0.01 and 0.05).

Fig. 12 presents plots of the holding capacity of the torpedo anchor, considering different values of the eccentricity parameter. This parameter was varied downwards and upwards from the value used on the main analysis (). The influence of this parameter on the determination of the anchor's holding capacity is notable through simple observation of the curves in Fig. 12. In general, as the value of the cap eccentricity parameter increases, the holding capacity estimated is more conservative. Furthermore, it can be noted that the curves converge to a "lower limit" for the pullout capacity as the eccentricity increases.

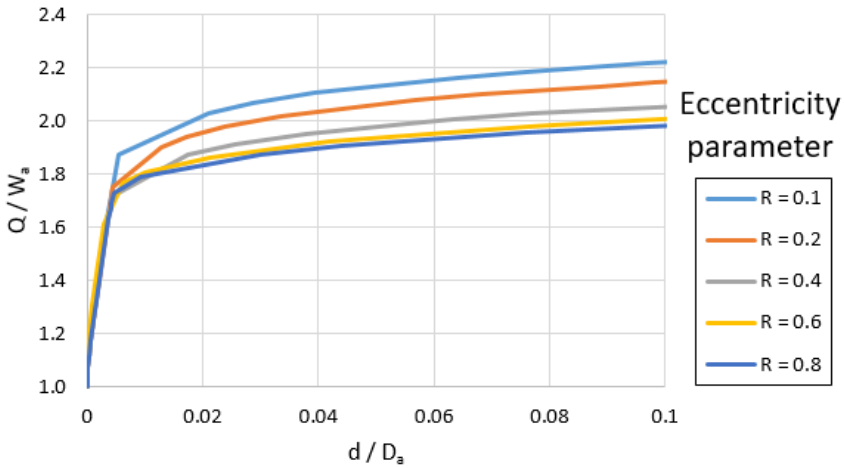


Figure 12. Influence of eccentricity parameter on pullout capacity.

## CONCLUSIONS

Numerical analyses were conducted in this study to evaluate the importance of considering setup effects on predicting the holding capacity of torpedo anchors. The investigations showed that the excess pore pressure dissipation represents the most crucial mechanism associated with the setup process, as was expected. During soil reconsolidation, a considerable increase in the effective stress at the anchor-soil interface could be observed and, consequently, an increase in shaft friction and anchor holding capacity.

The holding capacity of the finless torpedo anchor analyzed was found to be approximately 32% higher than its initial value, which is a considerable increase. Although the time needed for complete soil reconsolidation be over ten years, a reasonable amount of recovery is noticed after 150 days after anchor installation. Thereby, regarding the design phase, considering five months after anchor driving is somewhat found to be adequate for this kind of structure while being conservative.

The total time required to complete the setup process depends mainly on the coefficient of permeability of the soil, as shown in Fig. 9. Soils with very low permeability, such as clayey soils, total setup time can be orders of magnitude larger than for soils with high permeability, which is the case of sandy soils. In addition, when approximately 80% of the setup is complete, the time range needed to get an increase on the anchor response is substantially more extensive than the time required at the beginning of the process.

Another critical aspect observed about the influence of the permeability coefficient is that when increasing its value in one order of magnitude (multiplying by a factor of 10), the time needed to achieve a specified consolidation ratio of the soil decreases in the same proportion. The obtained value is not precisely the one received by applying a factor of 10, but it is very close to that.

The constitutive plasticity behavior of the soil was also analyzed through this study. Some of the cap model parameters were varied to understand their influence on structure's response. The flow stress ratio has almost no impact on the results, as shown in Fig. 10. On the other hand, transition surface and eccentricity parameters appear to have a more substantial influence on predicting the holding capacity of the torpedo anchor. Nevertheless, the results obtained are in good agreement, and the application of a safety factor could easily cover this influence.

## ACKNOWLEDGEMENTS

The study described in this paper results from a partnership between Petrobras and UFRJ and was carried out with resources from the R&D program of the Electricity Sector regulated by ANEEL, under the PD-00553-0045/2016 project titled "Planta Piloto de Geração Eólica Offshore".

The authors would also like to express their gratitude to "Fundação Carlos Chagas Filho de Amparo à Pesquisa do Estado do Rio de Janeiro" (FAPERJ) and to "Coordenação de Aperfeiçoamento de Pessoal de Nível Superior" (CAPES), for the resources destined to the production of this research.

## REFERENCES

Abaqus/CAE 6.13-1. Dassault Systèmes. 2013.

Abaqus 6.13 Online Documentation. Theory manual. Dassault Systèmes. 2013.

API. **Recommended Practice for Planning, Designing and Constructing Fixed Offshore Platforms – Working Stress Design (RP 2A-WSD)**. American Petroleum Institute, 20th ed., USA, 2005.

CARTER, J. P.; RANDOLPH, M. F.; WROTH, C. **Stress and pore pressure changes in clay during and after the expansion of a cylindrical cavity**. International Journal for Numerical and Analytical Methods in Geomechanics, vol. 3, pp. 305-322, 1979.

EHLERS, C. J. Ehlers; YOUNG, A. G.; CHEN, J. H. **Technology assessment of deepwater anchors**. Proceedings of the 36th Offshore Technology Conference, Houston, TX, 2004.

GIBSON, R.; ANDERSON, W. **In situ measurement of soil properties with the pressumeter**. Civil engineering and public works review, vol. 56, pp. 615-618, 1961.

HELWANY, S. **Applied soil mechanics with Abaqus applications**. John Wiley & Sons, Inc., Hoboken, New Jersey, 2010.

HILL, R. **The mathematical theory of plasticity**. Oxford University Press, 1950.

HOUSSAIN, M. S.; KIM, Y.; GAUDIN, C. **Experimental investigation of installation and pullout of dynamically penetrating anchors in clay and silt**. Journal of Geotech. and Geoenviron. Eng., 140(7), 2014.

HOUSSAIN, M. S.; O'LOUGHLIN, C. D.; KIM, Y. **Dynamic installation and monotonic pullout of a torpedo anchor in calcareous silt**. Géotechnique, 65(2), pp. 77-90, 2015.

KARLSRUD, K. **Prediction of load-displacement behavior and capacity of axially loaded piles in clay based on analyses and interpretation of pile load test results**. Doctoral thesis at NTNU, Trondheim, 2012.

KEAVENY, J. M.; MITCHELL, J. K. **Strength of fine-grained soils using the piezocone**. Use of In Situ Tests in Geotechnical Engineering (GSP 6), ASCE, Reston/VA, pp. 668-699, 1986.

KOMURKA, V. E.; WAGNER, A. B. **Estimating soil/pile setup**. Final Report, University of Wisconsin-Madinson, 2003.

LOPES, G. K. **Análise numérica da capacidade de cargas de âncoras torpedo considerando efeitos de setup**. Master thesis, Federal University of Rio de Janeiro, RJ, Brazil, 2019.

MEDEIROS JR., C. J. **Low cost anchor system for flexible risers in deep waters**. Proceedings of the 34th Offshore Technology Conference, Houston, TX, 2002.

RADGAHAR, E.; RAIE, M. S.; MOTAMANI, N. **Simulation of torpedo-shaped anchor (without fins) for submersible offshore platforms under tensile force**. Journal of Appl. Environ. Biol. Sci., 5(8S), pp. 107-111, 2015.

RAIE, M. S.; TASSOULAS, J. L. **Simulation of torpedo anchor setup**. Marine Structures, 49, pp. 138-147, 2016.

RANDOLPH, M. F.; WROTH, C. **An analytical solution for the consolidation around a driven pile**. Intenational Journal of Numerical and Analytical Methods in Geomechanics, vol. 3, pp. 217-229, 1979.

RICHARDSON, M. D.; O'LOUGHLIN, C. D.; RANDOLPH, M. F.; GAUDIN, C. **Setup following installation of dynamic anchors in normally consolidated clay**. Journal of Geotech. Geoenvirom. Eng., 135(4), pp. 487-496, 2009.

SIMULIA. **Analysis of driven pile setup with Abaqus/Standard**. Abaqus Technology Brief, 2007.

SOUSA, J. R. M. de; AGUIAR, C. S.; ELLWANGER, G. B. Ellwanger; PORTO, E. C.; FOPPA, D. **Undrained load capacity of torpedo anchors embedded in cohesive soils**. Journal of Offshore Mechanics and Arctic Engineering, 133 (2), 2011.

TERZAGHI, K. **The shearing resistance of saturated soils and the angle between the planes of shear**. Proceedings of the First International Conference on Soil Mechanics and Foundation Engineering, vol. 1, pp. 54-56, 1936.

WODEHOUSE, J.; GEORGE, B.; LUO, Y. **The development of a FPSO for the deepwater Gulf of Mexico**. Proceedings of the 39th Offshore Technology Conference, Houston, TX, 2007.

## ÍNDICE REMISSIVO

## V



## W

COLEÇÃO

# DESAFIOS DAS ENGENHARIAS:

## ENGENHARIA DE COMPUTAÇÃO 2

www.atenaeditora.com.br
contato@atenaeditora.com.br
@atenaeditora
www.facebook.com/atenaeditora.com.br

Atena Editora

Ano 2021

COLEÇÃO

# DESAFIOS DAS ENGENHARIAS:

## ENGENHARIA DE COMPUTAÇÃO 2

www.atenaeditora.com.br
contato@atenaeditora.com.br
@atenaeditora
www.facebook.com/atenaeditora.com.br

Atena Editora
Ano 2021